

AD-A208 629

DTIC FILE COPY

④

FINAL REPORT

CONTRACT #N00014-88-CC-0611

BAND STRUCTURE ENGINEERING

FOR ULTRA-LOW THRESHOLD LASER DIODES

DTIC
ELECTE
MAY 22 1989
S D

DISTRIBUTION STATEMENT A
Approved for public release;
Distribution Unlimited

089 5 02 027

④

FINAL REPORT
CONTRACT #N00014-88-CC-0611
BAND STRUCTURE ENGINEERING
FOR ULTRA-LOW THRESHOLD LASER DIODES

Issued by
Office of Naval Research
Department of the Navy
800 N. Quincy Street
Arlington, Virginia 22217-5000

DTIC
ELECTE
MAY 22 1989
S D D

To
Ortel Corporation
2015 W. Chestnut St., Alhambra, CA 91803

1988
~~Contract Period:~~
~~88 Aug 31 88 Apr 30~~

RECEIVED
DEPARTMENT OF THE NAVY
ARLINGTON, VA

Band Structure Engineering for Ultra-low Threshold Laser Diodes

Final Report for Contract #N00014-88-C-0611

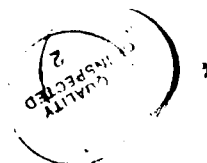
I. Ury and Kam Y. Lau

Ortel Corporation

2015 W. Chestnut St., Alhambra, CA 91803

1. Introduction

While semiconductor lasers of high level of sophistication and reliability have been developed for present day fiberoptic telecommunications, demands for ultralow lasing threshold and ultrahigh modulation speed stem mainly from applications involving relatively short distance interconnections within a computer. The need for optics in computers arises from the increasing parallelism in modern computer architectures, which places heavy demands on input/output functions at gigahertz clock rates[1] (Fig. 1). Further considerations of using semiconductor lasers in computer optical interconnects shows that conventional semiconductor lasers are unacceptable for such purposes[2], the main problem being that they must be biased at or above lasing threshold for proper modulation behavior. This mode of operation requires a monitor photodiode and an active feedback circuit to stabilize the operating point. In a supercomputer where there are as many as a few hundred thousand interconnections, such feedback circuits will occupy a large amount of real estate and the bias current required will consume an unacceptable amount of power. It is therefore far



Date	
Dist	Speed
A-1	

OPTICAL INTERCONNECT

1ST LEVEL—FRAME—→FRAME CAN BE ACCOMPLISHED
WITH STANDARD LASER AND RECEIVER MODULES

2ND LEVEL—BOARD—→BOARD $\sim 10^5 - 10^6$ CONNECTIONS IN A
SUPERCOMPUTER

3RD LEVEL—ON BOARD (CHIP—→CHIP)

4TH LEVEL—ON CHIP

- PRACTICAL IMPLEMENTATION OF 2ND AND 3RD LEVEL
INTERCONNECT

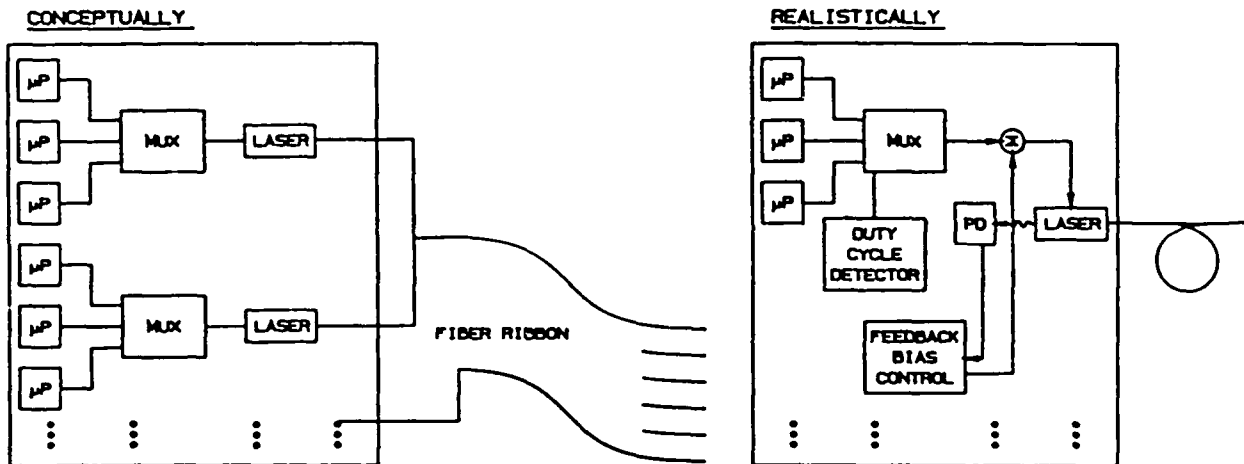


Fig. 1 Schematic diagram of a scheme for optically interconnecting high speed computers.

preferable that the laser diodes used in computer interconnects be driven directly by logic level signals without any need for biasing and stabilization. However, it is well known that lasers modulated in this manner suffer from three drawbacks : (1) a substantial delay between the onset of lasing and the current pulse; (2) severe relaxation oscillation in the optical pulse; and (3) pattern effect as a result of charge left-over from the previous pulse(s) (Fig. 2). Direct digital switching of laser diodes without current prebias also allows fully ON-OFF switching. An analysis of the switching dynamics of semiconductor lasers showed that these problems can be solved by using a very low threshold laser with threshold of less than 1mA.

The concept of "optical interconnect" in supercomputers has matured to the point where it is very important that devices with the above mentioned characteristics be available for actual implementation of interconnect schemes. Recent work has resulted in ultra-low lasing threshold GaAs lasers using quantum well structures[3]. The basic physics of the limiting factors was clarified and this led to the first demonstration of a sub-milliampere threshold laser, with the lowest being 0.55mA[4]. The realization of the superlow threshold is in part due to the use of single quantum well materials, and in part due to the use of an advanced laser structure, the buried heterostructure. A version of the basic structure, the window buried heterostructure, was developed[5] as a means to attain ultra-high modulation speeds of beyond 10GHz. In a related front, there were studies on possible means

FOR MASSIVE DEPLOYMENT OF LASERS WITHIN SUPERCOMPUTERS FOR INTERCONNECTS

($\sim 10^5$ CONNECTIONS)

- MONITOR PHOTODIODE AND FEEDBACK
CONTROL FOR INDIVIDUAL LASERS
HIGHLY UNDESIRABLE/UNACCEPTABLE
- NEED SIMPLE DRIVE FORMAT
- DRIVE LASER DIRECTLY WITH DIGITAL PULSE
NO FEEDBACK-CONTROLLED PREBIAS TO LASER

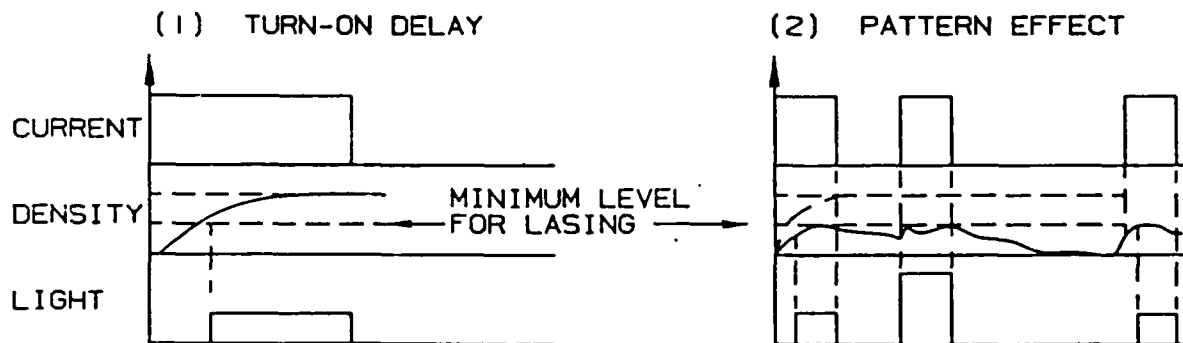


Fig. 2 Problems encountered when driving a laser diode without appropriate biasing.

to increase the modulation bandwidth of lasers to 30GHz using quantum well structures[6]. Theoretical predictions show that an appropriately designed multi-quantum well laser shows a factor of 2-3 increase in the modulation bandwidth over conventional lasers.

Looking forward to the next generation of semiconductor optoelectronic devices, one particularly exciting approach is through band structure engineering which can lead to order-of-magnitude improvements in the threshold of semiconductor lasers. It has been predicted that by suitably modifying the semiconductor band structure, notably the valence band effective mass, lasing thresholds as low as $10\mu A$ can be obtained, which is a whole order of magnitude lower than the best laser today. Past studies have shown that the basic limiting mechanism to obtaining low lasing threshold is the transparency condition, which is the electron density required for the material to become optically transparent. The transparency condition is attained when the quasi-Fermi level separation is equal to the bandgap. If the effective mass of the hole is very large, which is the common case in GaAs, the density of states is correspondingly large and the number of carriers required to fill these states in order to bring the Fermi level to that required for inversion is large. Thus it can be said that the present transparency condition, whether in conventional or in quantum well lasers, is dominated by the hole effective mass, and if it can be lowered by

artificial means to that near the electron effective mass, then improvements in lasing threshold of an order of magnitude will result. These points will be illustrated in detail in a later section.

A further consequence of lowering the effective mass of the holes is that the differential optical gain - the increase in optical gain per increase in the electron density - is also enhanced. This is not an obvious result, but which will come out of the analysis that follows. It also turns out that the direct modulation bandwidth of a semiconductor laser is proportional to the square root of the differential gain, so that lowering the effective mass of holes will result in a higher modulation speed as well. This gain in modulation speed, however, is not universal for devices of any construction, but only for those with the appropriate device length and reflectivities. We will analyze these issues in the following.

Modification of the effective mass of holes can be accomplished by changing the band structure of the crystal which is effected by a strained layer quantum well structure. Ordinarily a material cannot be grown on a substrate unless their lattice constants match very closely. However, a superlattice can be made out of two semiconductors with substantially different lattice constants as long as the individual layers of the constituents are sufficiently thin and the difference between the lattice constants is such that the strain energy is smaller than the misfit dislocation energy[7,8]. The strain between the layers

under these conditions is accommodated coherently (without dislocations). The first order effect of biaxial strain is a modification of the bandgap. In general, compressive strain widens the bandgap and tensile strain narrows the bandgap. Changes are more profound in the valence band due to the presence of heavy and light hole bands which ordinarily are degenerate at zone center, as shown in Fig. 3. Under biaxial compressive strain, new bands emerge which are admixtures of the heavy and light hole bands, with the uppermost band having a lighter mass in the direction parallel to the layer and a heavier mass perpendicular to it. Under biaxial tensile strain, the opposite is true. The former is a more favorable situation for laser action. The desired biaxial compressive strain can be found in InGaAs layers grown on GaAs substrate, which can produce lasing action at wavelengths of around $1\mu m$.

2. Optical gain in semiconductor lasers

Before we analyze strained quantum well lasers it is useful to review the basic gain mechanism in laser diodes in general. The state of a forward biased junction is given by the quasi-Fermi levels of the electrons and holes, and the electron and hole densities are given respectively by

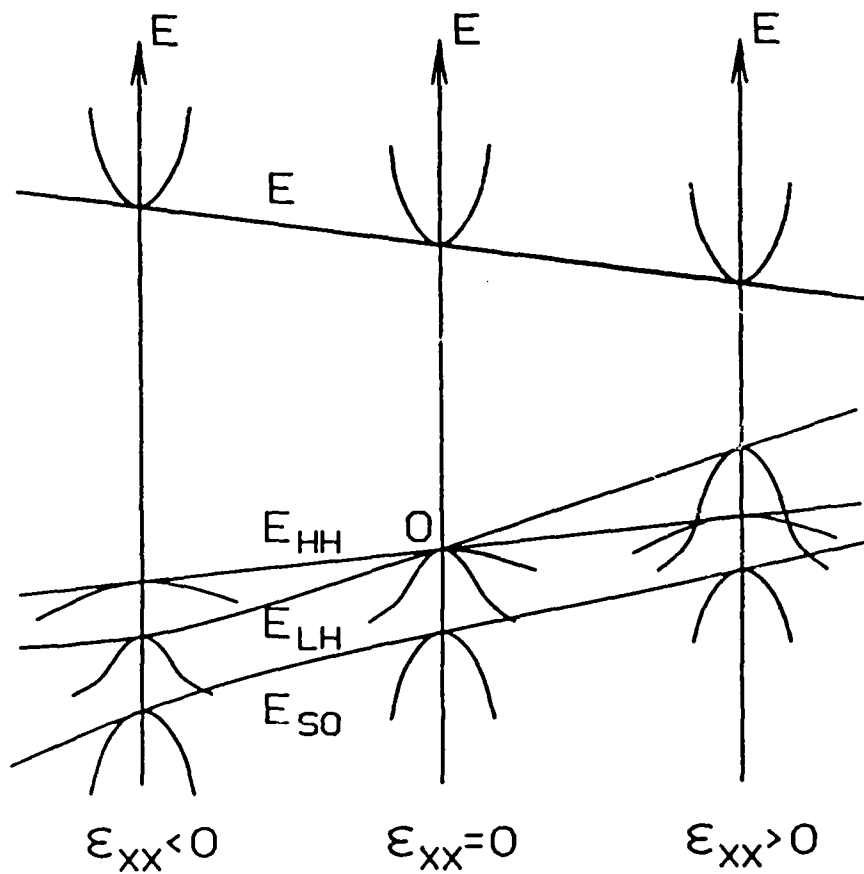


Fig. 3 Schematic representation of the band structure of III-V compound under uniaxial strain and stress.

$$n = \int \rho_c(E_c) f_c(E_c, E_{fc}) dE_c \quad (1)$$

$$p = \int \rho_v(E_v) f_v(E_v, E_{fv}) dE_v \quad (2)$$

where

$$f_c(E_c, E_{fc}) = \frac{1}{\exp(E_c - E_{fc}) + 1} \quad (3)$$

$$f_v(E_v, E_{fv}) = \frac{1}{\exp(E_v - E_{fv}) + 1} \quad (4)$$

are the Fermi distributions with E_c measuring positive into the conduction band from the conduction band edge, and E_v measuring positive into the valence band from the valence band edge. The quantities $\rho_{c,v}$ are the density of state functions, which in a conventional (three dimensional) material is proportional to the square root of the energy, and assumes a staircase shape in an ideal quantum well. In general, though, due to the interactions between different bands and the non-parabolicity of the bands, the density of states functions assume forms more complicated than the simple staircase model. The optical absorption coefficient, with k-selection rule enforced, in the parabolic band approximately, is

$$\alpha(E) = \xi \rho_r (1 - f_c - f_v) \quad (5)$$

where

$$E = \hbar\omega - E_g = E_c + E_v \quad (6)$$

is the reduced photon energy, ξ is a material constant, and E_g is the effective bandgap of the quantum well material, which is the sum of the bandgap of bulk GaAs, the lowest quantization energies of the electrons and that of the holes. The quantity $\rho_r(E)$ is the reduced density of states, which in the three dimensional case is given by

$$\frac{1}{\rho_r} = \sum_i \left(\left(\frac{1}{\rho_c} \right)^{2/3} + \left(\frac{1}{\rho_{ui}} \right)^{2/3} \right)^{3/2} \quad (7a)$$

where the summation is over the numerous hole bands, and in the two dimensional quantum well case, considering the energetically lowest quantized states only,

$$\frac{1}{\rho_r} = \sum_i \left(\frac{1}{\rho_c} + \frac{1}{\rho_{ui}} \right) \quad (7b)$$

The choice on whether to enforce the k-selection rule depends on the material under consideration: for heavily doped compounds the transition is dominated by bandtail states where k-selection rule does not apply; on the other hand in lightly doped quantum well materials k-selection should apply, as experimental data seem to indicate. The gain coefficient $g(E)$ is simply the negative of the absorption coefficient. For the material to experience gain at some photon energies, $g(E) > 0$ for at least some E , which from Eq. (5) gives the following condition:

$$\frac{1}{\exp[(E_c - E_{fc})/kT] + 1} + \frac{1}{\exp[(E_v - E_{fv})/kT] + 1} > 1 \quad (8)$$

which can then be further reduced to

$$E_{fc} + E_{fv} > E_c + E_v \quad (9)$$

This is the well-known Bernard-Durauffourg condition for optical transparency in a semiconductor. The electron density (and hence the injection current) needed to attain this point can be found by finding E_{fc} and E_{fv} subjected to the condition Eq. (9) and simultaneously the charge neutrality condition, $n=p$.

The electron density for transparency represents a fundamental limit to achieving the lowest lasing threshold. The current needed for lasing in general composed of two parts - the first part being the current needed for maintaining the electron density at the optical transparency level, and beyond that a second part to attain the necessary gain to overcome all the losses in the laser cavity. It can be argued (and can actually be done experimentally) that a laser cavity can be designed such that the losses are minimal, but this can only reduce the second part of the threshold current while the first part, that responsible for optical transparency, is unaffected. The key to building an ultralow threshold laser is thus to design a laser cavity with a very low loss, with a material that has the lowest transparency electron density. A single quantum well structure is one that possesses both of these qualities, and when combined with high reflectivity coating to minimize mirror loss, results in the lowest threshold on record today[4].

It can be shown that the lowest transparency electron density will result when the density of states functions of the electrons and holes

are both small and identical. Unfortunately this is not the case in most III-V materials, in which the effective mass of the hole (which is proportional to the power 2/3 of the hole density of states in 3-D materials) is an order of magnitude larger than that of the electron effective mass. Consider the case when the electron and hole density of states functions are identical in functional form and that the hole density of states is D times that of the electron density of states, $\rho_v(E) = D\rho_c(E)$. Then charge neutrality gives the following:

$$\int \rho_c dE \left(\frac{1}{\exp(E - E_{fc})/kT + 1} - \frac{D}{\exp(E - E_{fv})/kT + 1} \right) = 0 \quad (10)$$

If $D=1$, then from symmetry, at the point of optical transparency $E_{fc} = E_{fv} = 0$. If $D>1$, then the integral contribution of the second term in the parenthesis in Eq. (10) must be reduced by requiring $E_{fv} < 0$ which forces $E_{fc} > 0$, thus resulting in a higher electron density.

3. Optical gain and direct modulation speed of a laser

While the optical gain inside a laser obviously has a direct influence on the threshold of the laser, what is not so obvious is that the differential optical gain has a direct influence on the modulation speed of the laser. To see this one starts with the basic description of laser dynamics which involves a pair of rate equations governing the photon and carrier densities inside the laser medium[9]:

$$\frac{dN}{dt} = \frac{J}{ed} - \frac{N}{\tau_s} - g(N)P \quad (11)$$

$$\frac{dP}{dt} = g(N)P - \frac{P}{\tau_p} + \beta \frac{N}{\tau_s} \quad (12)$$

where N is the carrier density, P the photon density in a mode of the laser cavity, J is the pump current, d the thickness of the active region, τ_s is the spontaneous recombination lifetime of the carriers, τ_p is the photon lifetime, $g(N)$ is the optical gain as a function of the carrier density, β is the fraction of spontaneous emission entering the lasing mode, and e is the electronic charge. The first rate equation states that the rate of increase in carrier density is equal to the rate of current injection, J/ed , less the rate of carrier loss due to spontaneous recombination, $(-N/\tau_s)$, less the loss the carriers due to stimulated recombination, $(-g(N)P)$. The second rate equation states that the rate of increase in photon density is equal to the rate of photon generation by stimulated emission $(g(N)P)$ less the loss of photons due to cavity dissipation $(-P/\tau_p)$ plus the rate of spontaneous emission into the photon mode $\beta N/\tau_s$. Equations (11) and (12) are simply a bookkeeping of the supply, annihilation and creation of carriers and photons inside the laser cavity and describe laser dynamics in a most basic manner. More detailed explanations of laser modulation behaviors can be obtained by addition and/or modification of the terms in Eq. (11) and (12). The steady state solution of Eq. (11) and (12) gives the familiar light versus current characteristics of a laser diode. To obtain information on the modulation dynamics of the laser, a small

signal analysis is performed on Eq. (11) and (12), a procedure which linearizes Eq. (11) and (12) about a steady state operating point. Writing

$$N = N_0 + ne^{i\omega t} \quad (13a)$$

$$P = P_0 + pe^{i\omega t} \quad (13b)$$

$$J = J_0 + je^{i\omega t} \quad (13c)$$

we separate the variables into the steady state part and a small sinusoidal part. Upon substitution into Eq. (12) and ignoring products of small terms, we obtain

$$i\omega n = \frac{j}{ed} - \frac{n}{\tau_s} - g'(N_0)P_0 n - g(N_0)p \quad (14a)$$

$$i\omega p = g'(N_0)P_0 n + \beta \frac{n}{\tau_s} \quad (14b)$$

This represents a conjugate pole-pair (second order low-pass filter) type of response, and the resonance frequency is approximately given by

$$f_r = \sqrt{\frac{g'(N_0)P_0}{\tau_p}} \quad (15)$$

The response drops off rapidly at 40dB/dec beyond the resonance frequency. The modulation bandwidth is therefore usually taken as f_r , which from Eq. (15) is proportional to the square root of the differential optical gain. Thus, when one considers the quantum well structure, one not only has to consider the transparency density, but the slope of the gain versus electron density relationship as well.

4. Optical gain in a quantum well structure

A quantum well laser consists of a very thin active layer, 200Å or less, in which the motion of electrons in the direction perpendicular to the well are confined to less than a de Broglie length and the allowable energies are quantized into distinct levels. The most important consequence of this quantization is the modification of the density of states function into a staircase like characteristic (Fig. 4). As one starts to pump electrons into a quantum well, the electron density builds up to a point where the material becomes optically transparent as in conventional bulk materials, and further increase in electron density brings about optical gain. The optical gain is considerably higher in a quantum well than in conventional bulk materials, but since its small physical dimension results in a very weak confinement of the optical mode, there is NO substantial overall advantage in a single quantum well as far as optical gain is concerned. The problem associated with a small optical confinement in quantum wells can be circumvented by using multiple quantum wells in the active region of a laser. On the other hand, since the electron density for transparency in a quantum well is approximately the same as that in bulk material (as we will show later), the small physical dimension of the former implies that a very tiny injection current is sufficient to bring it to transparency. A combination of a small current for

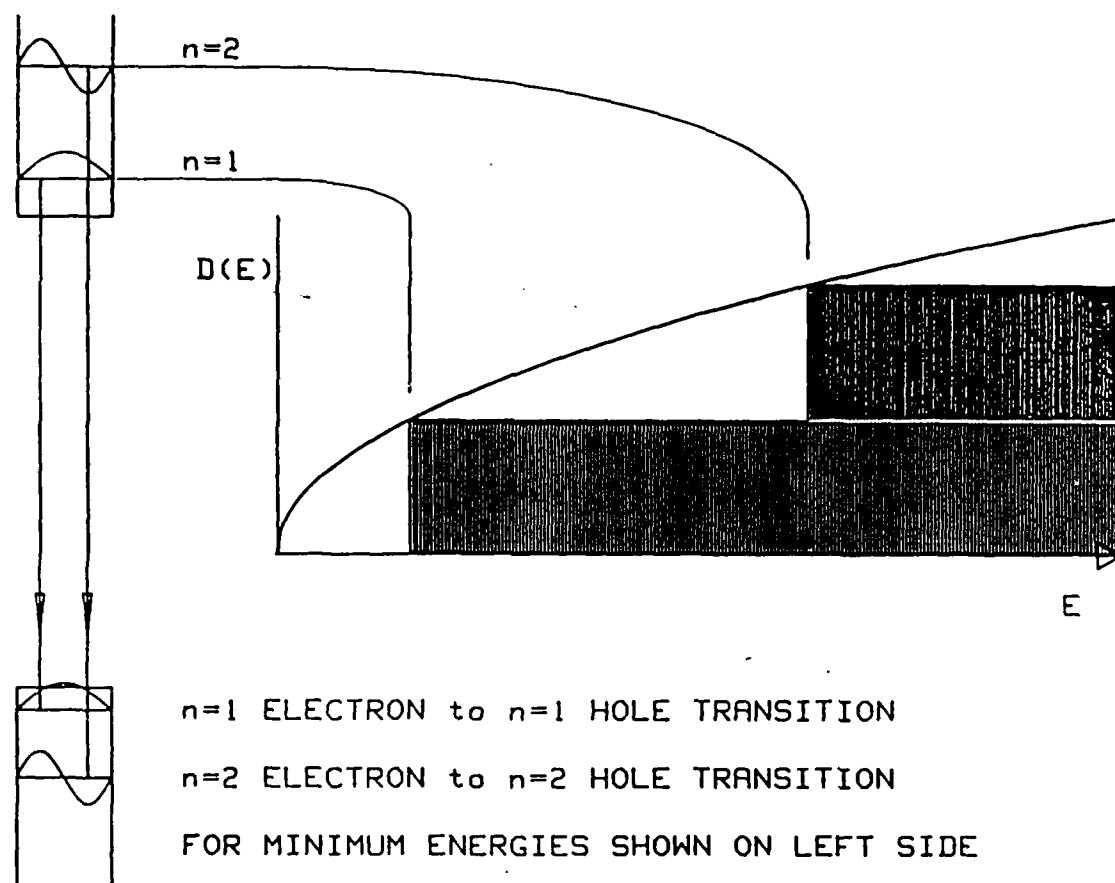


Fig. 4 Step-like density of states function of a two-dimensional quantum well (From Ref. 21).

transparency and a higher optical gain enable multi-quantum well buried heterostructure lasers to be built with threshold current as low as 2.5mA[10].

A significant result of the above discussion is that while a single quantum well laser does not have a very high optical gain, the transparency condition can be most easily reached compared to conventional or multiquantum well lasers. Optical gain is required in a laser for overcoming cavity (mirror and internal) losses, which can be readily reduced tenfold by increasing facet reflectivity to above 90% since the internal loss of a single quantum well laser is only about one-tenth of that of conventional double heterostructure. The current required for transparency is a fundamental quantity since it remains even when the cavity loss is reduced to zero. Thus the logical way to construct a laser with the lowest possible threshold is to use a single quantum well structure in a low loss cavity - a buried heterostructure (for efficient carrier confinement) single quantum well laser, with high reflectivity coatings.

It was mentioned above that one of the underlying reason for a low transparency density in quantum well lasers is that since the transparency electron density is approximately the same as that in bulk materials, the much thinner active region of a quantum well implies a much reduced transparency current. We will show here why the transparency electron density is nearly independent of well thickness,

and to what extent this holds true. Transparency occurs when the separation in quasi-Fermi levels equals the minimum separation in available valence and conduction band states, the Bernard-Duraffourg condition:

$$E_{fc} + E_{fv} = \epsilon_{v1} + \epsilon_{c1} \quad (16)$$

where E_{fc}, E_{fv} are the quasi-Fermi levels, measured from the band edges and positive into the bands as before, and $\epsilon_{fc}, \epsilon_{fv}$ are the first quantized energies in the conduction and valence bands, respectively. The electron and hole densities are given by

$$n, p = \int \rho_{c,v} f_{c,v}(E, E_{fc,v}) dE \quad (17)$$

where $f_{c,v}$

are the Fermi distribution as given in Eqs. (3) and (4), and $\rho_{c,v}$ are the conduction and valence band density of states functions, which in the simple constant effective mass, parabolic sub-band approximation is given by

$$\rho_c = \frac{m_c}{\pi \hbar^2 L_z} \sum_i H(E - E_{ci}) \quad (18)$$

where $H(x)$ is the Heaviside function, E_i is the i th quantized energy given in the infinite well approximation by

$$E_{ci} = \frac{i^2 \pi^2 \hbar^2}{2m_c} L_z^{-2} \quad (19)$$

and L_z is the width of the quantum well. Substituting Eq. (18) into (17) one obtains

$$n = \frac{m_c}{\pi \hbar^2 L_z} \sum_n E_{fc} - E_{nc} + kT \ln(1 + \exp((E_{nc} - E_{fc})/kT)) \quad (20)$$

A set of corresponding formulae exists for holes with the only addition that heavy and light holes are summed over in (18). The condition for charge neutrality equates n and p (for an undoped quantum well), and provides a relation between E_{fc} and E_{fv} . This together with the transparency condition Eq. (16) uniquely determines the Fermi levels and hence the electron density at transparency. The computed transparency electron sheet density is shown in Fig. 5. For comparison, the result for an infinite well is also shown. The transparency density decreases linearly with well thickness until approximately 100Å, and from then on stays approximately constant between 100Å and 50Å, at the latter point the electrons are no longer confined in the quantum well. Experimentally, a nearly constant threshold current dependence of a very long laser devices (which approaches the transparency current) on well width between 40 and 100Å was observed[11].

While it appears that lowering the thickness of a single quantum well to much below 100Å will not aid in lowering the transparency current, it has been proposed that further reduction can result from reducing the effective mass of the heavy hole band[12,13]. This is to be accomplished by strained layer structures, which is the topic of the next section.

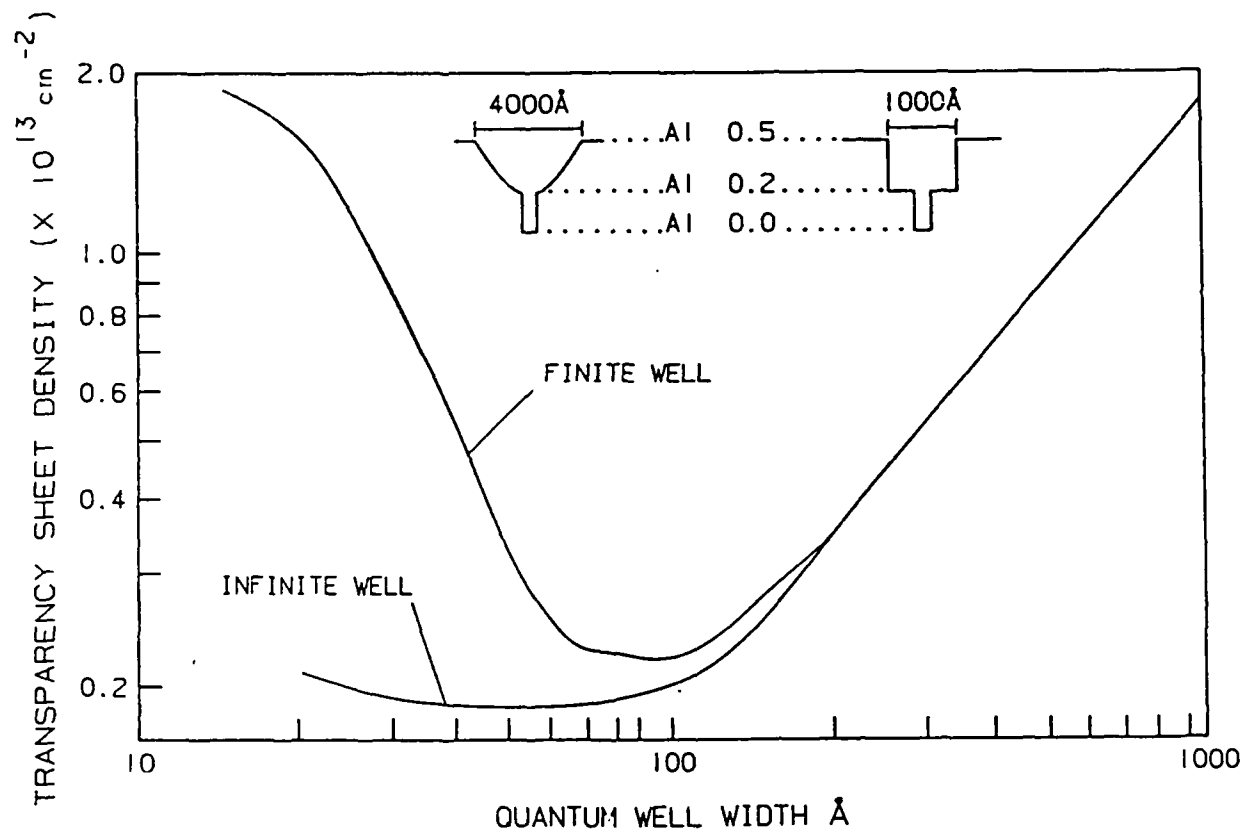


Fig. 5 Computed threshold current density as a function of well thickness for a single quantum well laser.

5. Strained layer quantum wells

It has been proposed that a strained layer superlattice be used to reduce the effective mass of holes, thereby reducing the transparency electron density and subsequently the lasing threshold. In conventional bulk materials, the degeneracy of heavy and light hole bands at the zone center means domination of the heavy hole band in hole occupation. It was known that by applying strain to the bulk crystal, the degeneracy can be broken such that under a biaxial compressive stress, the light hole band is lifted above the heavy hole band in the k -vector directions parallel to the applied strain (Fig. 3)[14]. Since the heavy hole is five times heavier than the light hole, the resultant effective hole mass can be reduced by a factor of 5. The strain can be built in by growing lattice-mismatched $\text{In}_x\text{Ga}_{1-x}\text{As}$ on a GaAs substrate. Such lattice-mismatched epitaxial layers cannot be arbitrarily thick for them to be defect free, the maximum thickness being only about 100Å for $x=0.2$. Thus all strained layer structures are by default quantum well structures, and it appears that the same argument above, that of lifting the light hole band above the heavy hole band by strain, can be applied to predict that strained quantum wells have an effective hole mass five times lower than that of unstrained quantum wells. This argument is largely incorrect, because in a regular quantum well, the lowest hole quantum state corresponds to the band which is heavy in the direction perpendicular to the well, and this same band happens to be light in the plane of the well. Hence the effective mass of the

lowest quantum state in a conventional quantum well is always that of a light hole, even without strain. This can be seen very clearly in band structure calculations of quantum wells; the valence subband structure of a $GaAs-Ga_{0.3}Al_{0.7}As$ quantum well in the (100) orientation is shown in Fig. 6 [15]. The question then becomes, what is the advantage of applying strain in a quantum well, since the effective hole mass is already so light? In fact, Shubnikov-de Haas measurements shows that the effective hole mass of a strained quantum well is reduced only by 20% below that of an unstrained quantum well[16], which is a minimal reduction in terms of influencing the threshold of a laser. The answer comes from a detailed examination of the band diagram Fig. 6, where it is seen that that the highest hole band, the HH1 subband, which has a hole mass of 0.2, deviates from the parabolic characteristic beyond approximately 10meV of the band edge, becoming substantially heavier as energy increases. This is very undesirable for laser operation, since under the heavy carrier concentration of $>10^{18}$ in common laser operation the hole energies extends well beyond 10meV into the band and effectively sees a very heavy mass. One can easily convert the band structure into a density of states function, and the non-parabolicity is reflected very clearly in Fig. 7[17], which shows a very low density at the band edge but increasing rapidly beyond. The non-parabolicity comes from the interaction between the subbands, and an applied strain can separate the bands further thus reducing the subband interaction, resulting in the parabolicity being maintained even deep into the band. (In addition, the narrower bandgap InGaAs

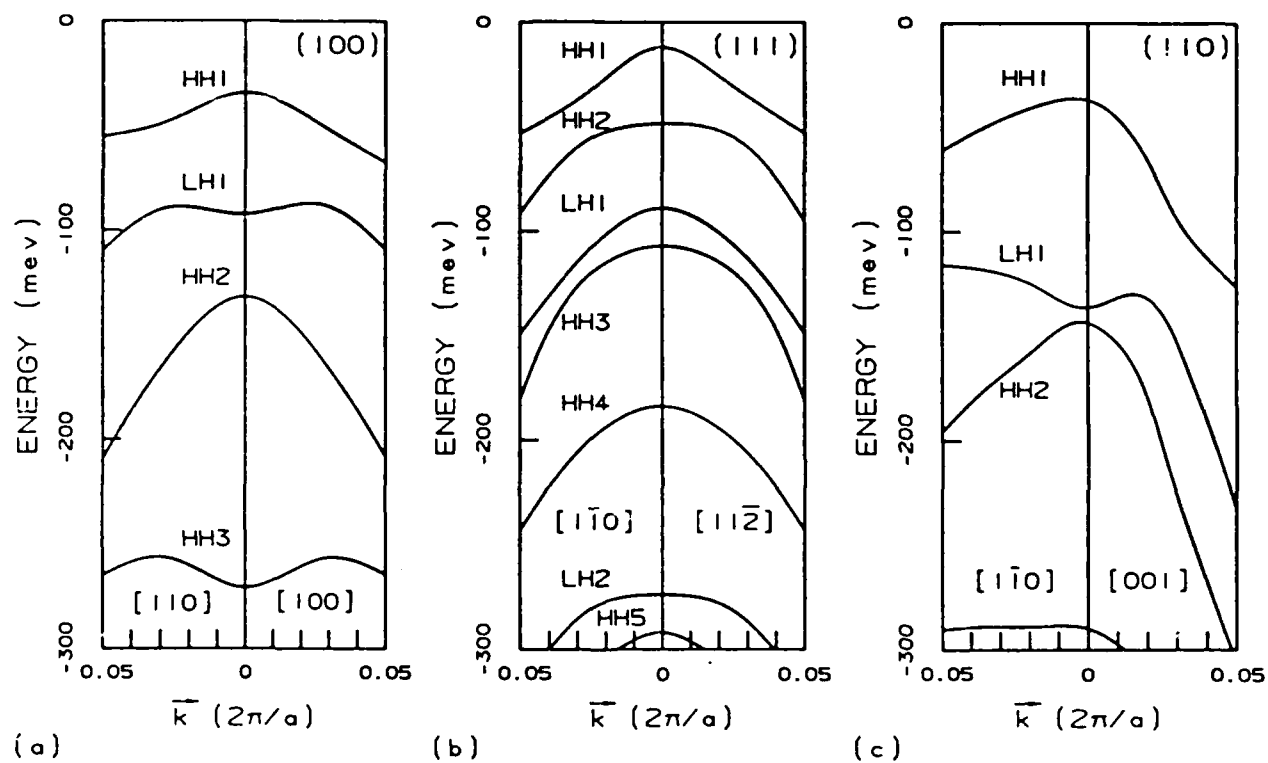


Fig. 6 Detailed structure of the hole bands of a single quantum well with various crystal orientations (From Ref. 15).

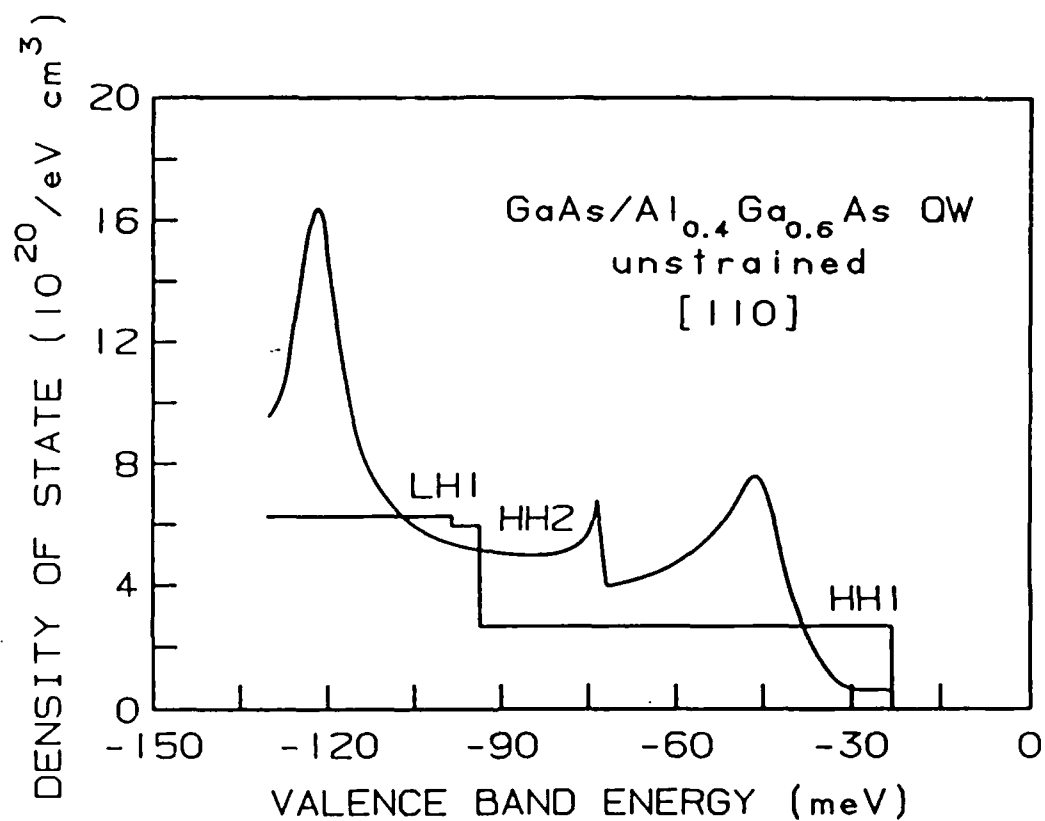


Fig. 7 Computed density of states function of a single quantum well. The staircase function is the ideal single quantum well density of states without taking into account the crystal orientation of the quantum well and band-to-band interaction (From Ref. 17).

leads to a lower hole mass to start with). This is illustrated in Fig. 8[17], where an almost flat density of states is maintained until the second hole band is encountered.

It is clear from the discussions in the above sections that a low density of states results in a low transparency electron density. What is not so clear is how a low density of states results in a higher differential gain - afterall, a low density of states means that at any particular photon transition energy there are fewer states available and hence the gain should be reduced. It will be shown that this is true only at very high carrier densities, and if one designs a laser which does not require a very high gain for lasing, the enhancement in differential gain is substantial. Strained layer lasers should therefore exhibit a higher modulation speed compared to a regular quantum well laser, provided that the laser parameters are properly designed.

The optical gain is given by

$$g(E) = \xi \rho_c (f_c + f_v - 1) \quad (21)$$

where

$$\xi = \frac{\hbar n q^2 |M|^2}{\epsilon_0 m_0^2 c \bar{\mu} E_{ph}} \quad (22)$$

is a material dependent parameter, $E_{ph} = \hbar \omega$ is the photon energy, and f_c, f_v are the Fermi factors

$$f_{c,v} = \frac{1}{\exp[(E_{c,v} - E_{fc,fv})/kT] + 1} \quad (23)$$

As before, the energies are measured positive into the conduction band from the (quantized) conduction band edge and positive into the valence from the valence band edge. For a quantum well in the constant effective mass approximation whose density of states are independent of energy, the reduced density of states ρ_r is the harmonic mean of the electron and hole density of states:

$$\frac{1}{\rho_r} = \frac{1}{\rho_c} + \frac{1}{\rho_v} = L_z \bar{h}^2 \pi \left(\frac{1}{m_c} + \frac{1}{m_v} \right) \quad (24)$$

For transitions with k-selection rules enforced, the electron and hole energies are related by

$$E_{c,v} = E \frac{m_r}{m_{c,v}} = \frac{\rho_r}{\rho_{c,v}} \quad (25)$$

The quasi-Fermi levels are related to the electron and hole densities by

$$n, p = \int \rho_{c,v}(E_{c,v}) f_{c,v}(E_{c,v}, E_{fc,fv}) dE_{c,v} \quad (26)$$

which can be evaluated for a constant density of state (as in the case of strained layer quantum for energies below 100meV, Fig. 8) to give

$$n, p = \rho_{c,v} \{ E_{fc,fv} + kT \ln(1 + \exp(-E_{fc,fv}/kT)) \} \quad (27)$$

Let the hole density of states be D times that of the electron density of states. Then, equating n and p under the charge neutrality condition yields the following relation between E_{fc} and E_{fv} :

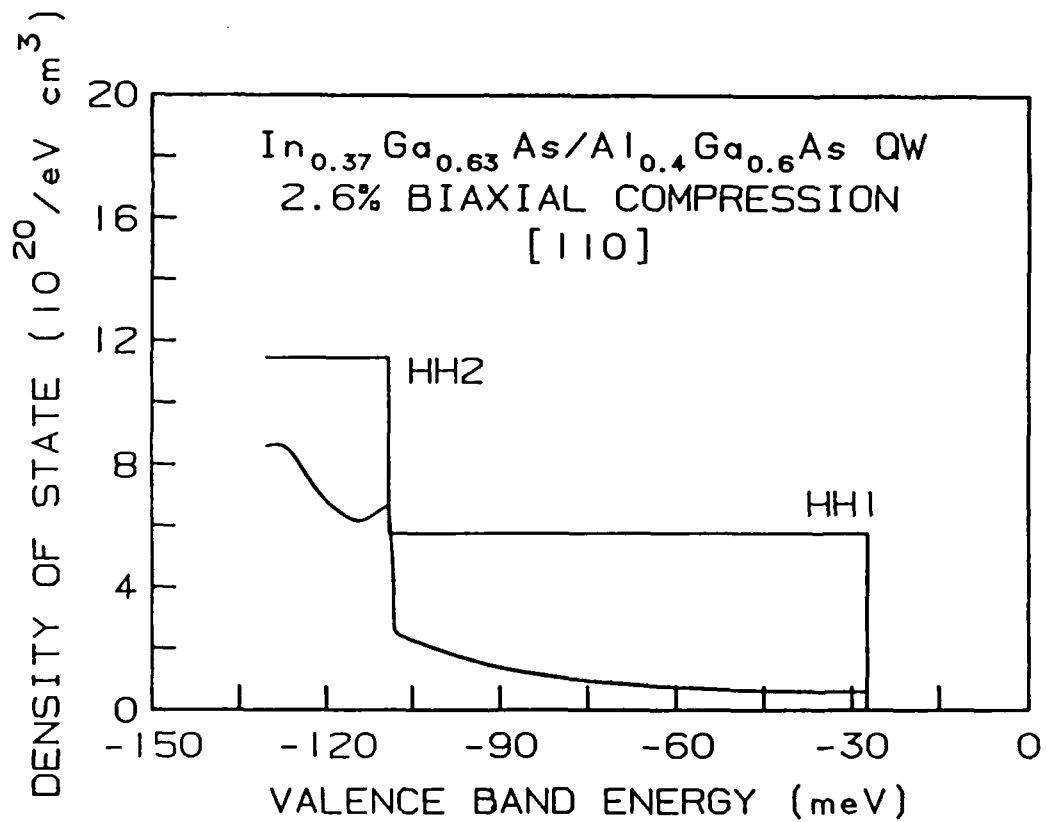


Fig. 8 Computed density of states of a strained quantum well with 2.6% biaxial strain (From Ref. 17).

$$(e^{E_{fc}/kT} + 1)^D = e^{E_{fv}/kT} + 1 \quad (28)$$

The gain spectrum of the strained quantum well is thus

$$g(E) = \xi \rho_r \left(\frac{1}{1 + e^{(E_c - E_{fc})/kT}} + \frac{1}{1 + e^{(E_v - E_{fv})/kT}} - 1 \right) \quad (29)$$

It can be easily seen that the maximum of this gain curve occurs at $E=0$, i.e., $E_c = E_v = 0$. Thus the maximum gain g_m is given by

$$g_m = \xi \rho_r \left(\frac{1}{1 + e^{-E_{fc}/kT}} + \frac{1}{1 + e^{-E_{fv}/kT}} - 1 \right) \quad (30)$$

which, using Eq. (28), can be converted to a relation that contains only a single variable, the electron quasi Fermi level:

$$g_m = \xi \rho_r \left(\frac{1}{(e^{E_{fc}/kT} + 1)^{1/D}} + \frac{1}{e^{E_{fc}/kT} + 1} - 1 \right) \quad (31)$$

It has been shown that the carrier lifetime in a quantum well structure is almost inversely proportional to the carrier density n , with the experimentally obtained dependence approximated by $\tau = (2.5 \times 10^9 \text{ s} \cdot \text{cm}^{-3})/n$ [18], from which the injection carrier density can be estimated for a given n . Using Eq. (27) and (31) one can plot the maximum gain versus the injected current density, as shown in Fig. 9, for various values of D . It will be assumed throughout this calculation that the electron mass is unchanged, while D is varied by varying the hole mass. The current density where g_m crosses zero is the transparency level, and decreases with decreasing D as expected. The maximum achievable gain is also reduced for small D , but this won't be felt

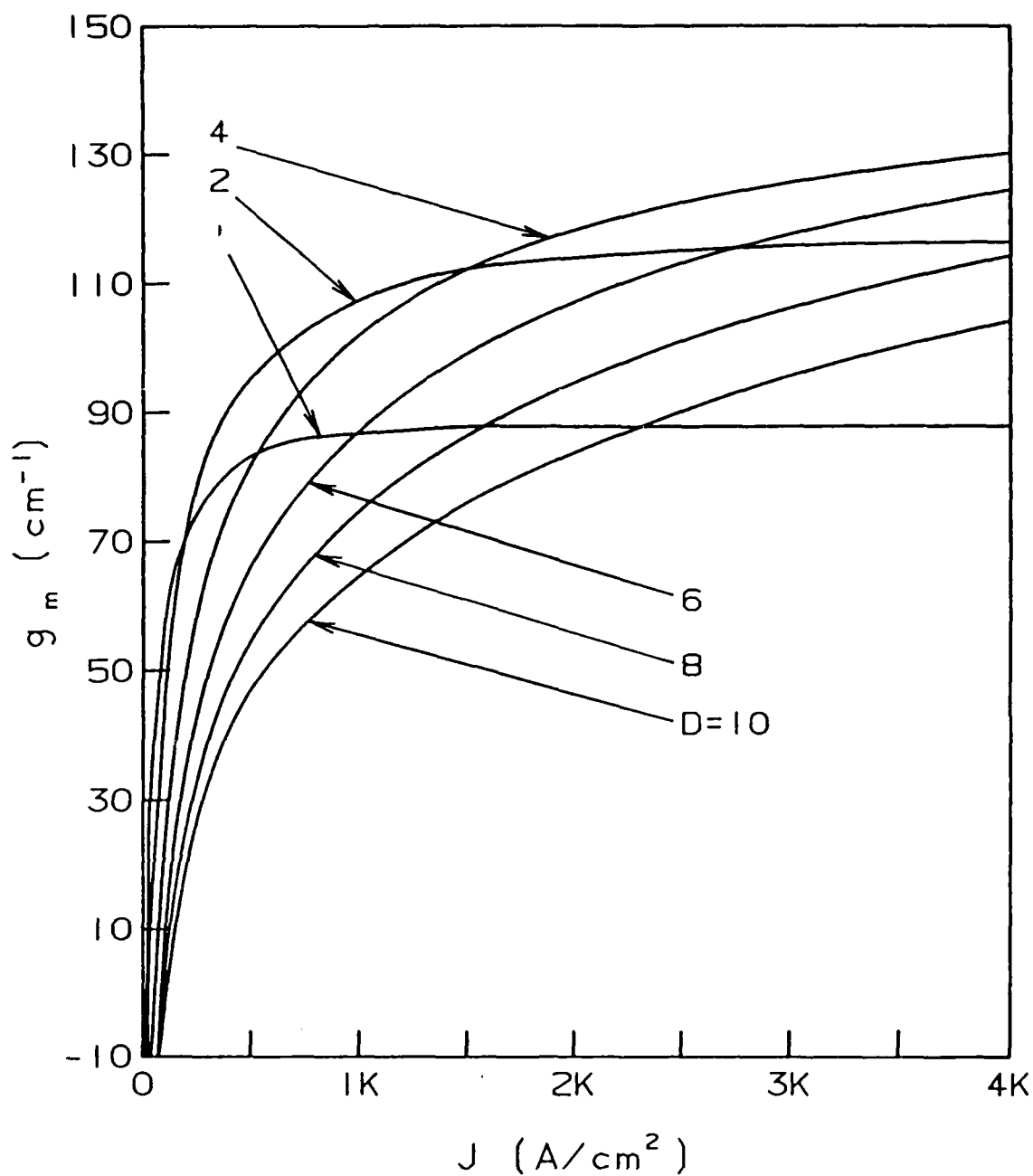


Fig. 9 Computed mode gain versus current density for a single quantum well with the electron density of states equal to that of a regular single-quantum well, while the hole density of states is D times that of the electron density of states.

until one reaches injection current densities of approximately 2.5 kA/cm^2 or higher.

As described previously, a very important parameter is the differential gain, dg_m/dn . A closed form solution can be obtained for strained layer quantum well by using the approximation Eq. (27) and (31):

$$\frac{dg_m}{dn} = \frac{dg_m}{dE_{fc}} \cdot \frac{dE_{fc}}{dn} \quad (32)$$

where

$$\frac{dg_m}{dE_{fc}} = \frac{\xi \rho_r e^{E_{fc}/kT}}{kT} \left(\frac{1/D}{(e^{E_{fc}/kT} + 1)^{1/D+1}} + \frac{1}{(e^{E_{fc}/kT} + 1)^2} \right) \quad (33a)$$

and

$$\frac{dn}{dE_{fc}} = \frac{\rho_c}{kT} \left(1 - \frac{1}{e^{E_{fc}/kT} + 1} \right) \quad (33b)$$

so that

$$\frac{dg_m}{dn} = \frac{\xi}{\rho_c + \rho_v} \left(\frac{\rho_c}{(e^{E_{fc}/kT} + 1)^{1/D}} + \frac{\rho_v}{e^{E_{fc}/kT} + 1} \right) \quad (34)$$

Fig. 10 shows plots of dg_m/dn as a function of g_m .

The relaxation oscillation frequency of the laser is given by

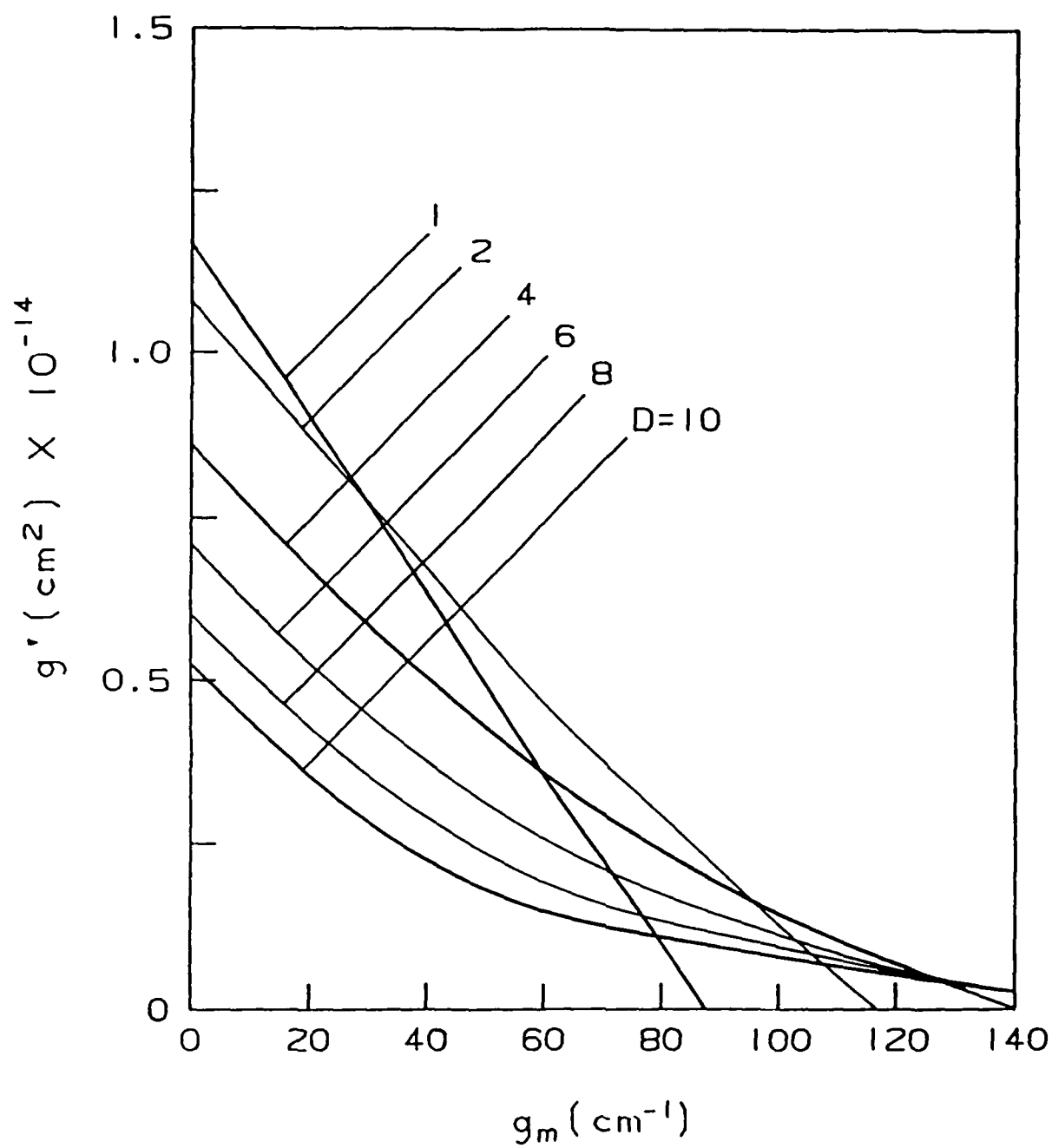


Fig. 10 The differential gain versus the peak gain for various D's.

$$f_r = \frac{1}{2\pi} \sqrt{\frac{c}{n_r} \frac{P_0}{\tau_p} g'} \quad (35)$$

where we denote dg_m/dn by g' , n_r is the refractive index and c is the velocity of light. The photon lifetime is related to the peak gain by

$$\frac{1}{\tau_p} = \Gamma \frac{c}{n_r} g_m \quad (36)$$

and hence the relaxation oscillation frequency is given by

$$f_r = \frac{1}{2\pi} \frac{c}{n_r} \sqrt{\Gamma g_m g' P_0} \quad (37)$$

The important quantity is thus the product $g_m g'$. Fig. 11 plots f_r against g_m for different values of D , at the same photon density P_0 . One striking feature of this plot is that the relaxation oscillation frequency of a regular quantum well laser (D in the order of 10) is quite independent of g_m , while that of a strained layer ($D=2$ or 1) shows a clear maximum. Thus by fitting actual modulation data to theory, one can actually obtain an estimation of the value D , the ratio of the hole to electron density of states, and hence the amount of strain in the quantum well. The plot also shows that the optimum value of D is actually around 2, at which point the relaxation oscillation frequency can be enhanced by a factor of approximately 1.5 by applying strain. Notice also that, in practical cases of strained InGaAs on GaAs strain structures, the bandgap is lowered and hence the lasing

wavelength is increased by up to 25% over GaAs, and therefore if one were to compare the modulation speed at the same optical power, the enhancement is even higher.

6. Experimental results

As mentioned in previous sections, the original motivation of using strained layer superlattices for lasers is its potential for order-of-magnitude reduction in threshold current over conventional quantum well lasers. Recent demonstrations of single quantum well lasers have achieved impressive results, with the lowest threshold current density to date at $<100\text{A}/\text{cm}^2$ [19], and the lowest threshold current for a "complete" device at 0.55mA [4]. These threshold currents are at such a low level that factors originating from device imperfections, such as junction leakage, existence of non-radiative recombination centers and waveguide imperfections, come to play a dominant role in determining the threshold current. Any additional, fundamental reduction of the threshold current by strained layer effects may be overwhelmed by such imperfections that they may not be realizable in practice. Thus by observing the threshold current alone, it is very difficult to verify the fundamental advantages offered, in theory, by strained layer structures. Recent experimental results on strained layer lasers[20] shows respectable threshold current densities, comparable to typical

quantum well lasers, but no better. There is thus no evidence that any of the predicted advantages of strained layer laser structures is real or not.

The analysis of previous sections on the modulation properties of strained layer lasers shows substantial deviation from that of regular quantum well lasers (which is substantially different from regular double heterostructure lasers). In particular, when one plots the relaxation oscillation frequency f_r versus the required gain for lasing, as in Fig. 11, one finds that for a single quantum well laser f_r is a very weak function of threshold gain (which is related to the device length and the mirror reflectivities), whereas for strained quantum well lasers the functional dependence is considerably more drastic. In fact, strained quantum well lasers offers an advantage in modulation bandwidth, but only at certain ranges of threshold gain. The origin of this effect is the nature of the gain versus electron density characteristic. The relaxation oscillation frequency of the laser is only a function of the product $g \cdot (dg/dn)$ and hence measurement of f_r versus g provides a direct probe of the gain characteristic, regardless of the existence of leakage currents or recombination centers which would drastically affect the threshold current. (Note that recombination centers or leakage current effectively affects the carrier lifetime, which severely affects the threshold current but does not enter into the expression for the relaxation oscillation frequency at all [5].)

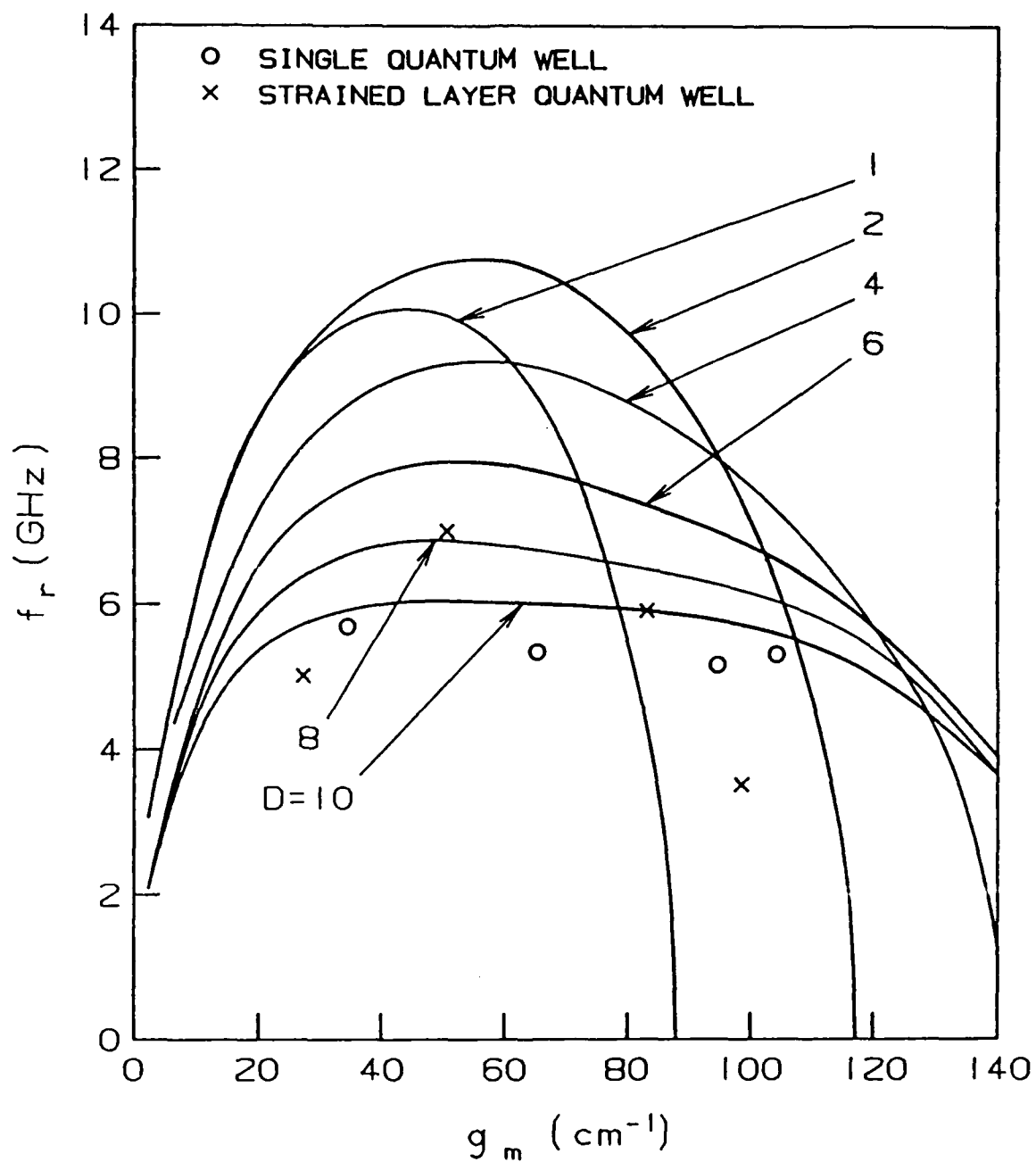


Fig. 11 Relaxation oscillation frequency versus peak gain for various D 's.

We experimentally compared the relaxation oscillation frequency of strained layer single quantum well lasers and regular single quantum well lasers. The regular single quantum well lasers were of a standard type with a graded-index cladding layer which were used for earlier experiments in low threshold current studies[4]. The strained layer single quantum well laser has a profile shown in Fig. 12, and was grown by molecular beam epitaxy at a substrate temperature of 600°C. With an indium concentration of approximately 20% in the active layer, layers with good surface morphology can be grown at a thickness up to 150Å. Stripe geometry lasers were fabricated with a stripe width of 7μm, and typical threshold current densities were around 1kA/cm². These values are considerably higher than typical single quantum well lasers.

The relaxation oscillation frequency of the lasers were observed on a standard microwave measurement setup[9]. Devices of various lengths were used, and the data points are superimposed on the theoretical plots of Fig. 11 for both single quantum well lasers and strained layer single quantum well lasers, operated at an identical optical power density per width of 3mW/μm. A striking feature one observes is that the relaxation oscillation frequency of standard single quantum well lasers is relatively independent of gain, while that for strained layer quantum well shows an obvious peak at an optical gain of around 60cm⁻¹. This observation is consistent with the theoretical expectations based on a reduced hole mass for the strained layer structure. In fact, for

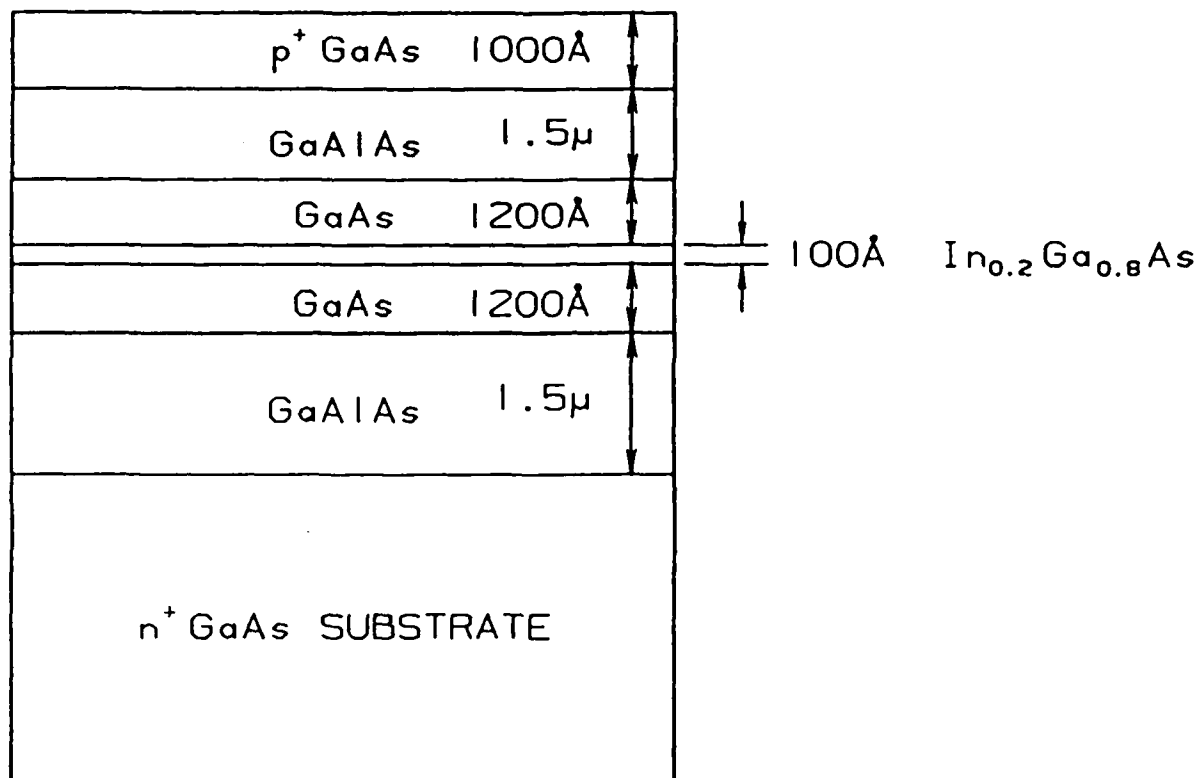


Fig. 12 Schematic structure of the strained single quantum well laser used in the experiment.

the present results, the observed peak of the relaxation oscillation versus gain characteristic matches that of the computed result for $D=2$. The overall observed relaxation frequency is lower than that predicted theoretically, this may be due to the uncertainty in estimating the optical power density at which the lasers are operating.

One last point that should be mentioned is that the present analysis considers optical transitions involving only the lowest quantized state. At high optical gains such as those above - depending on the transversal structure - 70 cm^{-1} , there is a possibility that the second quantized state transition is involved [21]. When this happens, one would expect in theory that the relaxation oscillation frequency experiences a sharp increase due to the higher differential gain of the second quantized state lasing at the transition. Fig. 13 shows the theoretically expected behavior of a regular 100 \AA single quantum well lasers calculated by using the parabolic band approximation from a large number of subbands and smearing of the density of states function [21,22]. The experimental data do not indicate any significant increase of the relaxation oscillation frequency with increasing gain up to 110 cm^{-1} . This could be due to a quantum well thickness substantially different than 100 \AA or less than perfect material quality. Even so the experimental findings reported in ref. 22 provide evidence that the model closely describes experimental conditions, taking proper account of the interband mixing that could produce a density of states function quite different from the simple smeared out

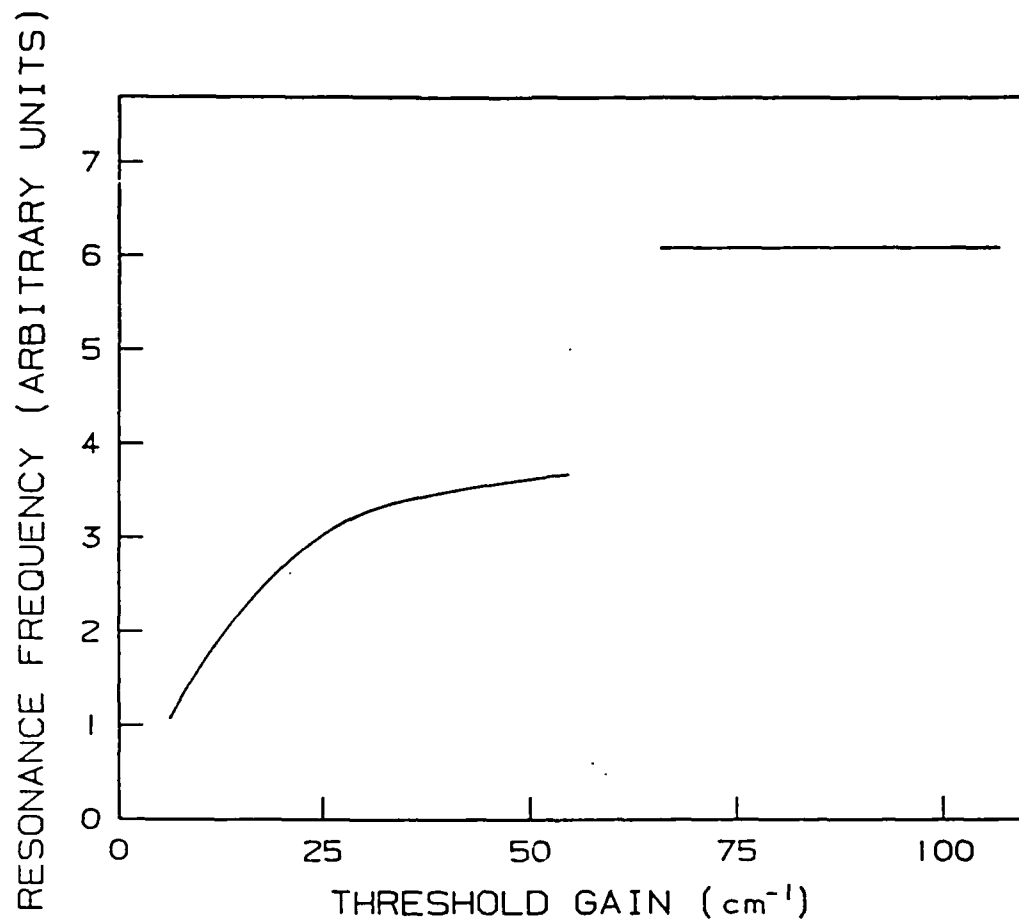


Fig. 13 Theoretical relaxation oscillation frequency versus peak gain, assuming a smeared out staircase density of states for a single quantum well and including contribution from the second and higher quantized state.

step function used in the model. In fact, one observes from Fig. 7 that when such interband mixing is taken into account, the density of states function of a regular quantum well is higher than that of the simple staircase, thus resulting in a higher available gain from the lowest quantized state than that predicted from the simple staircase model. To resolve these issues further investigations will be necessary.

7. Conclusion

It is shown that the unique properties of strained quantum well lasers can be identified by measuring the relaxation oscillation frequency of the lasers as a function of optical gain. These measurements exclude effects due to non-radiative recombinations and leakage currents, which can mask the beneficial effects in terms of a lower threshold current due to a reduced hole mass in strained quantum wells. The conclusion, both theoretically and experimentally, is that strained quantum well lasers have a higher differential gain, but which saturates at a lower gain level, as compared to regular quantum well lasers. The higher differential gain results in a higher relaxation oscillation frequency and hence a higher modulation speed. The saturation behavior is not necessarily a disadvantage, since such characteristics are needed for ultra-high speed mode-locking of semiconductor lasers[23], as well as other novel device application utilizing the non-linear effects of the optical gain. The results in this report are obviously only preliminary, and further studies in this area promise to create not

only lower threshold lasers as predicted previously, but also leads to novel optoelectronic device applications using the highly non-linear optical gain characteristics of strained layer quantum wells and superlattices.

References

1. J.W. Goodman, F.J. Leonberger, S.Y. Kung and R.A. Athale, Proc. IEEE, **72**, 850 (1984).
2. K.Y. Lau, Optical Processing Annual Review, Defence Advanced Research Project Agency, Washington D.C., Nov. 1985.
3. P.L. Derry, A. Yariv, K.Y. Lau, N. Bar-Chaim, K. Lee and J. Rosenberg, Appl. Phys. Lett., **50**, 1773 (1987).
4. K.Y. Lau, N. Bar-Chaim, P.L. Derry and A. Yariv, Appl. Phys. Lett., **51**, 69 (1987).
5. K.Y. Lau and A. Yariv, IEEE J. Quant. Electron., **QE-20**, 71 (1984).
6. Y. Arakawa and A. Yariv, IEEE J. Quant. Electron., **QE-21**, 1666 (1985); K. Uomi, T. Mishima and N. Chinone, "Ultra-high relaxation-oscillation frequency (up to 30GHz) of highly p-doped GaAlAs multi-quantum well lasers", Appl. Phys. Lett., **51**, 78 (1985).
7. J.W. Matthews and A.E. Blakeslee, J. Crystal Growth, **32**, 265 (1976).
8. P. Voisin, C. Delande, M. Voos, L.L. Chang, A. Segmuller, C.A. Chang and L. Esaki, Phys. Rev. B, **30**, 2276 (1984).
9. K.Y. Lau and A. Yariv, Semiconductors and Semimetals, Vol. 22B, Chp. 2, Academic Press, 1985.
10. W.T. Tsang, Appl. Phys. Lett., **39**, 786 (1981).
11. T. Hayakawa, T. Suyama, T. Kakahashi, M. Kondo, S. Yamamoto and T. Hijikata, IEDM'87, Washington D.C.
12. A.R. Adams, Electron. Lett., **22**, 250 (1986)

13. E. Yablonovitch and E.O. Kane, IEEE. J. Lightwave Tech., LT-4, 504 (1986).
14. G.C. Obsborn, IEEE. J. Quant. Electron., QE-22, 1677 (1986); J.E. Schirber, I.J. Fritz and L.R. Dawson, Appl. Phys. Lett., 46, 187 (1985).
15. M.P. Hounq, Y.C. Chang and W.I. Wang, J. Appl. Phys., 64, 4609 (1988).
16. Y. Iye, E.E. Mendez and W.I. Wang and L. Esaki, Phys. Rev. B, 33, 5854 (1986).
17. I. Suemune, L.A. Coldren, M. Yamaniski and Y. Kan, Appl. Phys. Lett., 53, 1378 (1988).
18. Y. Arakawa, H. Sakaki, M. Nishioka, J. Yoshino and T. Kamiya, Appl. Phys. Lett., 46, 519 (1985).
19. H.Z. Chen, A Ghaffari, H. Morbboc, and A. Yariv, Appl. Phys. Lett. 51, 2094 (1987).
20. S.E. Fischer, D. Fekete, G.B. Peak and J.M. Ballantyne, Appl. Phys. Lett., 50, 714 (1987).
21. M. Mittelstein, Y. Arakawa, A. Larsson, and A. Yariv, Appl. Phys. Lett. 49, 1689 (1986).
22. M. Mittelstein, D. Mehnys, A. Yariv, J.E, Ungar, and R. Sarfaty, Appl. Phys. Lett. 54, 1092 (1989).
23. K. Lau, Appl. Phys. Lett. 52, 2214 (1988).